

VIV Response Prediction for Long Risers with Variable Damping

Vivek Jaiswal

Department of Mechanical Engineering
Massachusetts Institute of Technology

Prof. J. Kim Vandiver

Department of Mechanical Engineering
Massachusetts Institute of Technology

ABSTRACT

This paper describes the Vortex Induced Vibration (VIV) response of long cylinders equipped with strakes and presents damping measurements from Gulf Stream Experiments conducted in October 2006. The experiments used a 500.4 foot (152.4 m) long composite pipe with an outside diameter of 1.43 inches (3.63 cm). The strakes were a triple helix design with a pitch to diameter ratio of 17.5. The pipe was equipped with varying amounts of strake coverage and was towed in the Gulf Stream which had current profiles which varied from nearly uniform to highly sheared. The measured response showed the characteristic of traveling waves. Modeling such response using mode superposition and Green's Function is presented.

INTRODUCTION

Modern steel catenary risers may exceed 3000 m in length and have length to diameter (L/D) ratios in excess of 4000. Most have partial strake coverage to protect them from VIV. Response to VIV and fatigue damage rate prediction for these risers is difficult because of high mode numbers and axially varying material and damping properties. The Gulf Stream Experiments conducted in October 2006 were designed to better understand the behavior of structures covered with strakes. Partial coverage with strakes and different configurations of coverage were tested. One of the major objectives was to gather data that can be used to calibrate and improve VIV prediction programs such as Shear7.

EXPERIMENT DESCRIPTION

The Gulf Stream Experiments of October 2006 were preceded by two similar experiments conducted in Lake Seneca, New York, in July 2004 and in the Gulf Stream in October 2004. The overall design of the experiment was similar to the

Gulf Stream Experiment of October 2004 [2]. The set-up for the experiment is shown in Figure 1.

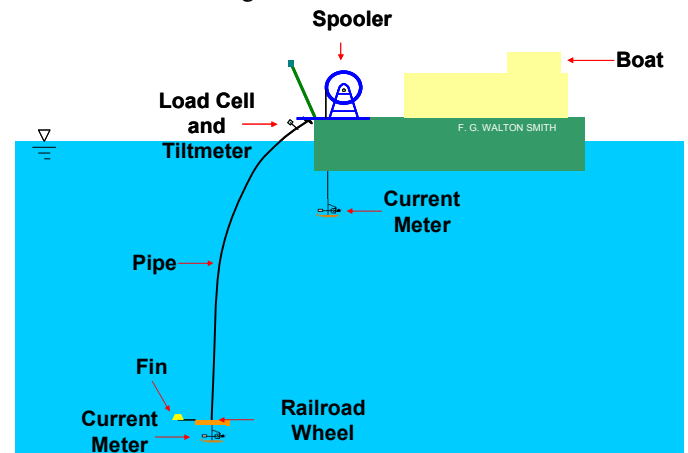


Figure 1. Set-up for the Gulf Stream Experiments 2006.

Gulf Stream Experiment 2006

The Gulf Stream Experiments were conducted on the Research Vessel F. G. Walton Smith from the University of Miami using a fiber glass composite pipe 500.4 foot long and 1.43 inches in outer diameter. The pipe was spooled on a drum that was mounted on the aft portion of the ship. The pipe was lowered directly from the drum into the water. A railroad wheel weighing 805 lbs (dry weight, 725 lbs in water), was attached to the bottom of the pipe to provide tension.

Strain gauges were used to measure the VIV response of the pipe. Eight optical fibers containing thirty five strain gauges each were embedded in the outer layer of the composite pipe. The gauges had a resolution of 1 micro-strain.

Two fibers were located in each of the four quadrants of the pipe, as seen in Figure 2.

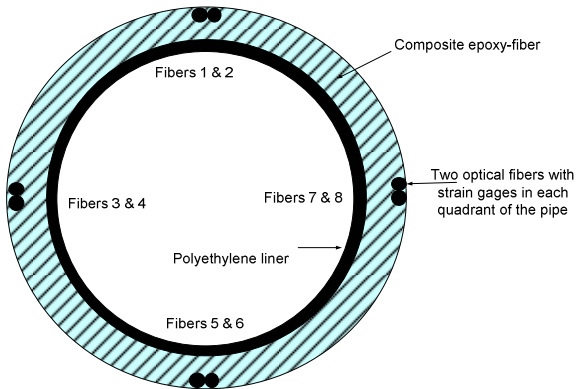


Figure 2. Cross-Section of the Pipe from the Gulf Stream Test.

The strain gauges in each fiber were spaced 14 ft apart and the two fibers in the same quadrant were placed such that their strain gauges were offset by 7 ft. This arrangement is shown in Figure 3.

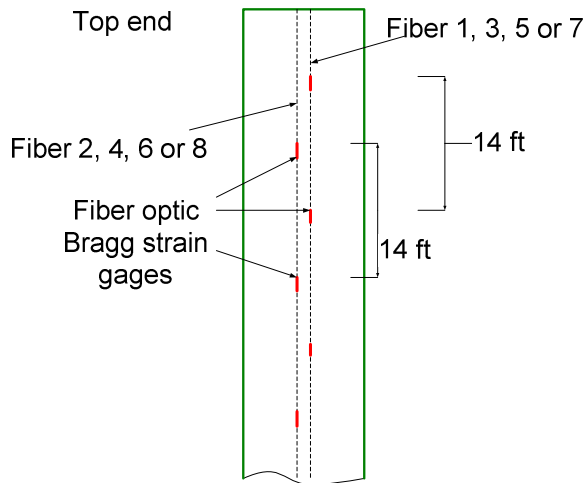


Figure 3. Arrangement of strain gauges in a quadrant.

The pipe properties are listed in Table 1.

Table 1. Gulf Stream Experiment 2006 pipe properties

Inner Diameter	0.98 in(0.0249 m)
Outer Diameter	1.43 in(0.0363 m)
Optical Fiber Position	1.37 in(0.0330 m)
EI	2.14e5 lb in ² (613 Nm ²)
Modulus of Elasticity (E)	1.33e6 lb/in ² (9.21e9 N/m ²)
EA	7.47e5 lb (3.32e6 N)
Weight in Seawater	0.133 lb/ft (flooded in Seawater) (1.942 N/m)
Weight in air, w/trapped water	0.511 lb/ft (7.46 N/m)
Effective Tension at the bottom end	725 lb, submerged bottom weight (3225N)
Material	Glass fiber –epoxy
Length	500.4 ft (152.4 m) (U-joint to U-joint)

The R/V F. G. Walton Smith is equipped with Acoustic Doppler Current Profilers (ADCP). During the experiments, the ADCP was used to record the current velocity and direction along the length of the pipe. Additional instrumentation included a tilt meter to measure the inclination at the top of the pipe, a load cell to measure the tension at the top of the pipe, a pressure gauge to measure the depth of the railroad wheel and two mechanical current meters to measure current at the top and the bottom of the pipe. The bottom current meter was suspended 6.56 ft (2 m) under the railroad wheel while the top current meter was suspended from the side of the boat and was 19 ft (5.8 m) below the free surface of the water.

EXPERIMENTS WITH STRAKES

During the Gulf Stream Experiments in October 2006, different strake coverage configurations and percentage coverage were tested. The strakes were a triple helix design with a pitch to diameter ratio of 17.5. The strake height was 25% of the diameter of the strake shell. The strakes were provided by AIMS International. The strake properties are listed in Table 2.

Table 2. Strake properties

Material	Polyethylene
Length	26.075 in (0.6623m)
Shell outer diameter	1.49 in (0.0378 m) including strake height
Shell inner diameter	1.32 in (0.0335 m)
Shell inner diameter when installed on the pipe	1.43 in (0.0363 m)
Strake height	0.375 in (0.0095 m), about 25% of shell outer diameter
Wall thickness	0.09 in (0.0023 m)
Pitch	17.5 times diameter
Weight per unit length in air	0.11 lb/ft ±10% (1.6 N/m ±10%)

The different configurations and coverage are schematically shown in Figure 4. The yellow lines in the figure represent strakes and the green lines represent bare pipe. In all seven different configurations were tested. These were:

1. 40% bottom end coverage. The strakes were applied in a two strakes followed by 10 inch gap configuration so that the actual coverage was 84% of the bottom 40% length of the pipe.
2. 25% coverage on both ends with 50% center pipe bare.
3. 50% center pipe coverage.
4. 50% staggered coverage.
5. 62% staggered coverage.
6. 84% staggered coverage.
7. 40% coverage at the bottom with an additional transition zone. The configuration for the transition zone is shown in Figure 5.

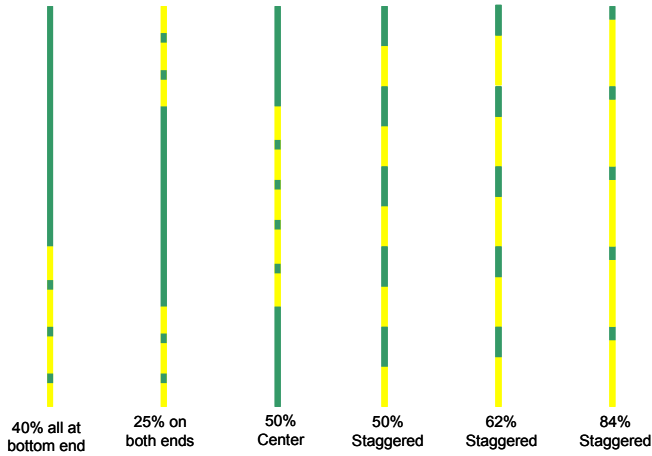


Figure 4. Strake coverage configurations.

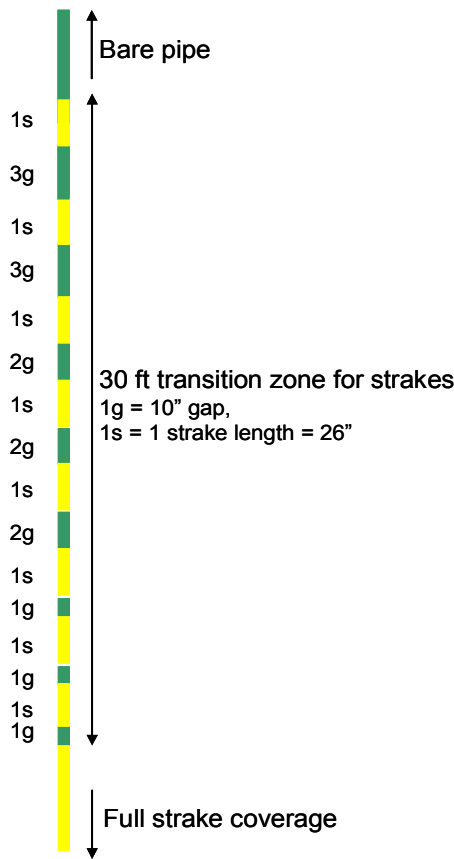


Figure 5. Strake transition zone.

DAMPING FOR STRAKES

The experiments with 40% strake coverage on the bottom end clearly showed that waves generated in the bare section traveled into the straked region and attenuate significantly

before reaching the ends. This can be seen in Figure 6 which shows the root mean square (RMS) bending strain for one of the tests (20061021213742) with 40% coverage on the bottom end. The four different colored stars represent data from each of the four quadrants. The strakes are present between the dimensionless axial coordinates (marked as relative position in the figures) of $x/L = 0$ to 0.4 . Relative position $x/L = 0$ in this figure as well as other figures presented in the paper corresponds to the bottom end of the pipe. Because of the high attenuation, there was no significant wave reflection from the bottom end. The waves in the straked region are traveling waves and an estimate of the damping present can be obtained by the log decrement method over the distance traveled [1].

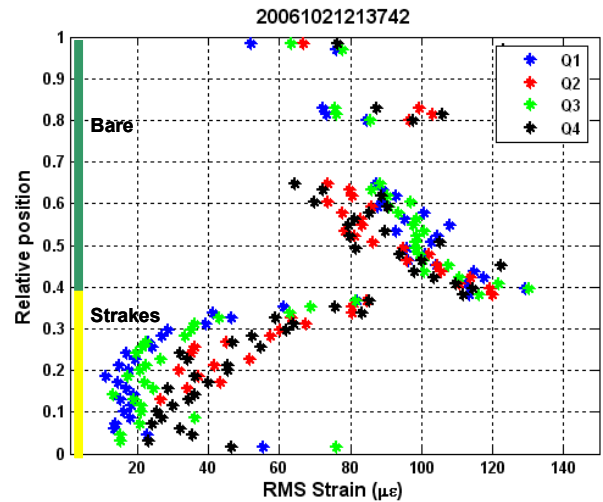


Figure 6. RMS Bending Strain for case 20061021213742. Data from all four quadrants is shown.

Figure 7 shows the power spectral density (PSD) of strains measured by two sensors located at an axial distance of 253.45 ft (77.25 m) from the top end of the pipe (relative position = 0.51) for the 40% coverage case. These sensors are located in the bare region. The two sensors measure strain in orthogonal directions and are nominally aligned with in-line and cross-flow directions. The primary shedding frequency (labeled as $1x$) can be seen in the PSD of strain in quadrant 3 while the two times the primary shedding frequency peak (labeled as $2x$) can be seen in quadrant 4. A broad three times peak (labeled as $3x$) can also be seen in the PSD of quadrant 3. The existence of higher harmonic ($3x$ peak) in experimental data has also been reported in [2] and [3].

The strain data was filtered so as to remove all the high frequency components and leave only the primary shedding frequency ($1x$) component. In order to get a damping estimate, an exponential curve is fitted to the RMS strain data in the straked region. The RMS strain at any point in the straked region (A) is related to the RMS strain at the beginning of the straked region (A_0) by the following equation:

$$A = A_0 e^{-k\zeta x}$$

where k is the wavenumber and ζ is the damping ratio and x is the distance between the two points along the axis of the pipe.

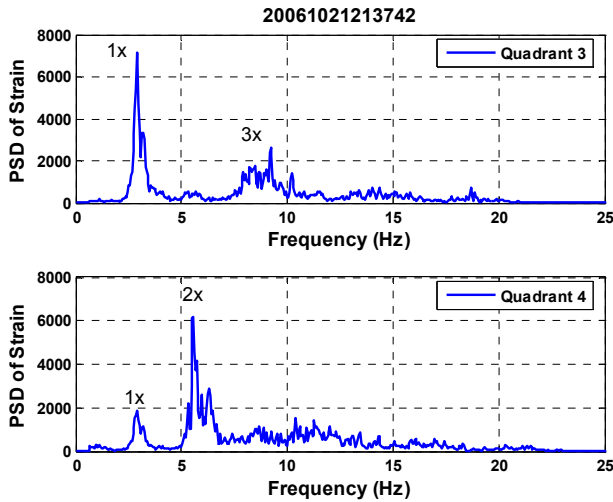


Figure 7. PSD of Strain at sensors located at an axial distance of 253.45 ft from top end. The sensors are in the bare pipe region.

Figure 8 shows an example of such a curve fitting. The RMS strain data corresponds to the primary response (1x) frequency. The higher frequency components have been filtered out.

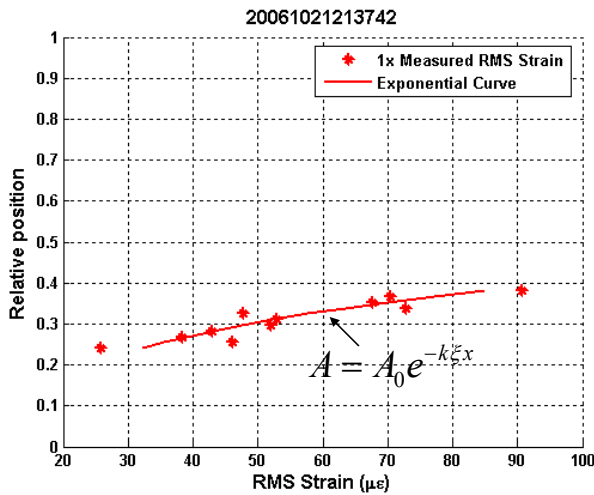


Figure 8. RMS Bending Strain in Straked Region and Exponential Curve fitted to the Data.

Figure 9 shows the estimated $k*\zeta$ values from seven different test data. The pipe under tension behaves like a string. The transverse wave propagation speed was found to be $c_z = 118$ ft/s in the straked region. The speed was determined by

measuring the phase shift between sensors a known distance apart. Using the formula

$$k = 2 * \pi * f / c_s$$

where f is the wave frequency in Hz, we can estimate the wavenumber k and hence obtain ζ values.

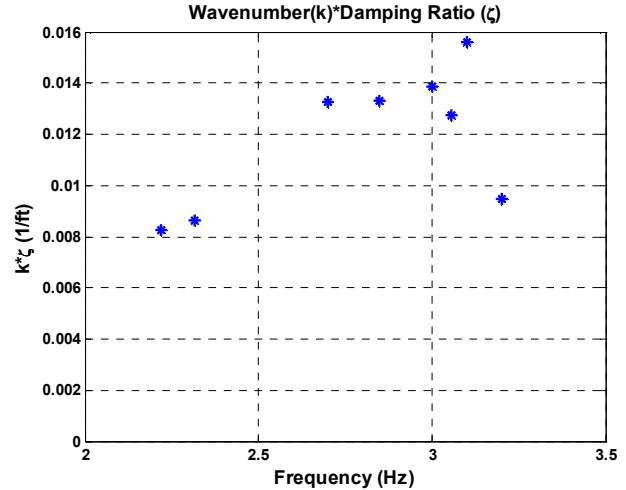


Figure 9. $k\zeta$ values for the strakes tested during the Gulf Stream Experiments 2006.

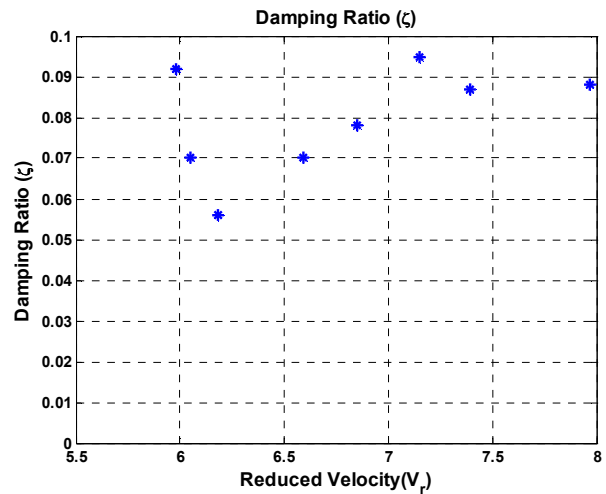


Figure 10. Damping Ratio (ζ) vs. Reduced Velocity for the strakes tested during the Gulf Stream Experiments 2006.

Figure 10 shows the estimated damping ratio plotted against the reduced velocity (V_r). The reduced velocity is given by

$$V_r = \frac{U_{mean}}{f_1 d}$$

U_{mean} is the mean value of the normal incidence current values at the sensor locations that were used for exponential curve fitting. f_1 is the primary response frequency and d is the diameter of the bare pipe. The damping ratio varied from 0.06 to 0.10 with a mean value of 0.08 for these tests.

MODELING STRAKES

Mode superposition and Green's Functions are well known tools for dynamic modeling of structures. In this paper the two methods will be used to model the response of the pipe tested during the Gulf Stream Experiments. Data from the experiment numbered 20061021213742 will be used as an example. In this experiment, the bottom 40% of the pipe was covered with strakes. The strakes were applied in the following pattern: two strakes followed by 10 inch gap resulting in an effective coverage of 84% on the bottom 40% length of the pipe.

40% Strake Coverage Tests

During the 40% strake coverage tests, the bottom 40% percent of the pipe (relative position 0 to 0.4) was covered with strakes. Figure 6 shows the measured RMS strain response from one of the cases. The main features of this response are:

1. A stress concentration at the point where the strakes begin.
2. Rapid decay of strain in the straked region.
3. The strain in the bare region is less than for a completely bare pipe for similar current profiles.[4]

The strakes proved effective because the region covered with strakes did not allow energy from hydrodynamic forcing to enter the system. The straked region always dissipated energy which entered the system through the bare region. This is an important point which must be kept in mind when modeling strakes.

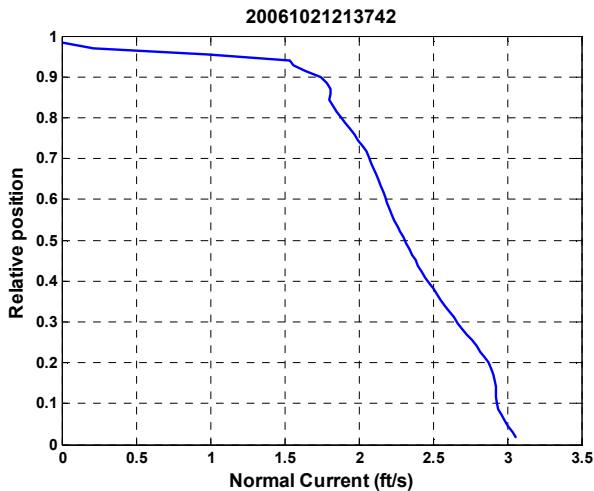


Figure 11. Normal incidence current profile for case 20061021213742.

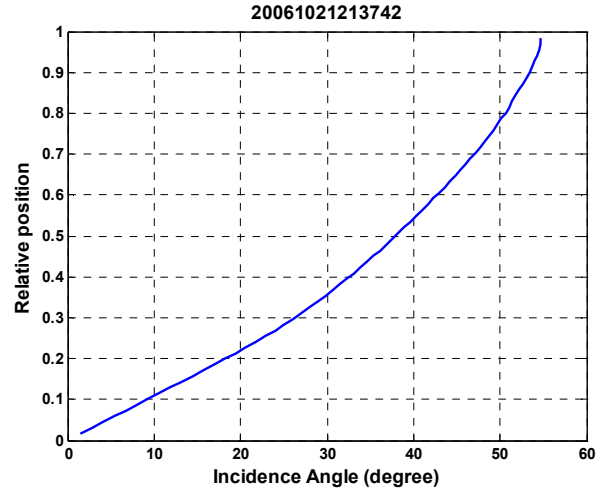


Figure 12. Angle of incidence of current for case 20061021213742.

Figure 11 shows the normal to the pipe axis component of the incident current for case 20061021213742. The profile has almost linear shear. Figure 12 shows the angle of incidence of current for the same case. It was found that regions with an angle of incidence greater than 47 degrees measured relative to the vertical never acted as power-in regions.

Mode Superposition Method

Mode superposition is a widely used method for predicting the dynamic response of structures. The method is fairly successful in predicting response of uniform or nearly uniform structures responding at low node numbers. However, for structures that respond at high mode numbers (greater than tenth mode) such that the waves in the structure are traveling waves and not standing waves, the method may have limited success. The mode superposition method models traveling wave behavior by including a large number of non-resonant modes. Ideally all the excited non-resonant modes must be taken into account but for practical purposes only a finite but sufficiently large number of non-resonant modes are used.

A key objective of this section is to reveal the inadequacy of the mode superposition method for modeling damping. An important feature of the method is that it averages local variations in damping over the entire length of the structure. This happens because of the definition of modal damping. Modal damping is defined as follows:

$$c_n = \int_{L_{power-out}} c(x)\Phi_n^2(x)\omega_n dx \quad (1.1)$$

where c_n is the modal damping coefficient for mode number N , $c(x)$ is the local damping coefficient, $\Phi_n(x)$ is the mode shape of mode N and ω_n is the natural frequency for mode N . Consider the two damping curves C1 and C2 shown in Figure 13. Curve C1 may qualitatively represent bare pipe damping whereas C2 may represent a case where the bottom portion of the pipe is

partially covered with strakes. The excitation or the power-in region is assumed to have no hydrodynamic damping while the remaining region dissipates energy (power-out region). If it is assumed that the integral in Equation (1.1) yields the same answer for both the curves then mode superposition will model the effects of damping in exactly the same way in both the cases.

A designer must therefore pay careful attention to these points when using mode superposition for response prediction for structures covered with strakes.

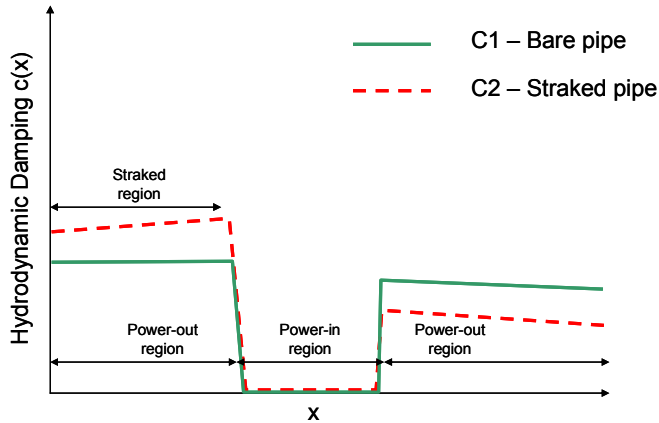


Figure 13. Illustration of qualitative variation in hydrodynamic damping along the length of pipe. C1 may represent the damping along a bare pipe and C2 may represent the damping along a pipe partially covered with strakes on one end.

The VIV prediction program Shear7 uses the mode superposition method. It is used in this paper to demonstrate the points mentioned above. Shear7 version 4.5 which implements time sharing has been used for all simulations presented in this paper. The concept of time sharing assumes that all the potentially dominant modes respond sequentially in time. The final response is the weighted mean in time of the individual modal responses. In the simulations presented in this paper, an equal weightage is given to all the modes i.e. each mode is assumed to respond for equal duration of time. Shear7 incorporates both structural and hydrodynamic damping in its damping calculation. Hydrodynamic damping is modeled using Venugopal’s model [5], [6]. The model needs three coefficients: K_{sw} , C_{vl} and C_{vh} as inputs.

Strain and current data from the 40% strake coverage case 20061021213742 is used to compare the predicted and measured response. The pipe under tension behaves like a string. The string model with pinned-pinned ends and uniform tension is used to model the pipe in Shear7. The pipe is divided into 3 zones as follows:

Zone 1: extends from relative position 0 to 0.4 and represents the straked region at the bottom end of the pipe. Since this region always behaves as a damping or power-out region, it is assigned a low Strouhal number (0.02) so that Shear7 never assigns any excitation force to this region. It should be noted that assigning a low Strouhal number to this zone does not affect the hydrodynamic damping computed by Shear7 for this zone. The added mass coefficient is assigned 1.5 for this zone to account for the increased added mass for the straked region. The hydrodynamic diameter is assumed to be the same as the bare pipe diameter.

Zone 2: extends from relative position 0.4 to 0.85 and represents the region through which the excitation energy enters the system. Based upon the measured response frequency in field, this region is assigned a Strouhal number of 0.16 and a reduced velocity bandwidth of 0.4. Since the flow is sheared, all potentially excited modes are allowed to participate in the response. The lift coefficient is estimated based upon the local reduced velocity from table 2 of the COMMON.CL file of Shear7. The table is an implementation of Gopalkrishnan data [7].

Zone 3: extends from relative position 0.85 to 1 and represents the region near the top end which cannot act as an excitation region because of the high angle of incident current. Like Zone 1, it is assigned a low Strouhal number for the same reason. Other properties like mass and damping are kept the same as those assigned to the bare pipe of Zone 2.

Two approaches of modeling the damping of the strakes and its effects are presented.

Approach 1: In this case, the coefficients describing the hydrodynamic damping in the straked region (Zone 1) are adjusted so that the modal damping ratio achieved for each of the potentially excited modes is between 0.06 and 0.10 ($K_{sw} = 0.40$, $C_{vl} = 0.36$ and $C_{vh} = 0.40$). This corresponds to the damping ratio measured for the straked region. The cutoff value of modal power ratio for selecting the potentially excited modes is kept low (0.1) so as to allow most of the potentially excited modes to participate in the response prediction.

Figure 14 shows the predicted strain response and compares it with the measured strain response corresponding to the primary response frequency. Only the primary response frequency component is considered because Shear7 does not yet account for the contributions coming from higher frequency components. The excited mode numbers are twenty to twenty eight. This approach yields a good match with the strain decay rate in the straked region but the overall predicted strain is below the measured strain. This happens because the high damping of straked region has been applied over the entire length of the structure as a modal damping.

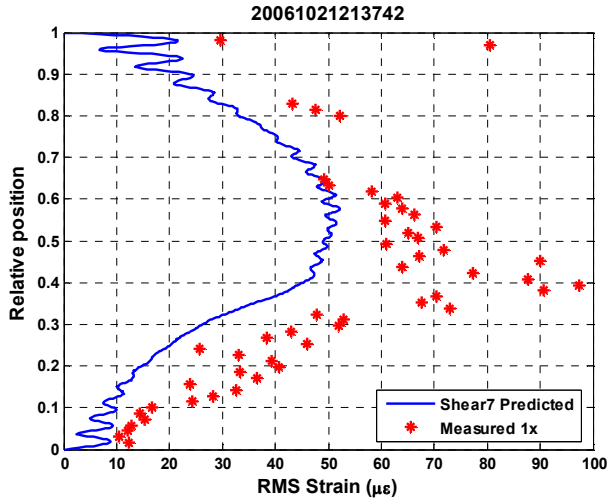


Figure 14. Shear7 v4.5 predicted response using approach 1.

Approach 2: In this case, the coefficients describing the hydrodynamic damping in the straked region (Zone 1) are adjusted so that the overall predicted response is similar to the measured response ($K_{sw} = 0.20$, $C_{vl} = 0.18$ and $C_{vh} = 0.20$). The cutoff value of modal power ratio for selecting the potentially excited modes is kept low (0.1) so as to allow most of the potentially excited modes to participate in the response prediction.

Figure 15 shows the predicted response and its comparison with the measured response. The excited modes are twenty to twenty nine. The modal damping ratio for the excited modes in this case varies between 0.03 and 0.07. The damping ratio estimated by fitting an exponential curve in the predicted response in straked region gives a damping ratio of 0.05 which is lower than the mean measured value of 0.08.

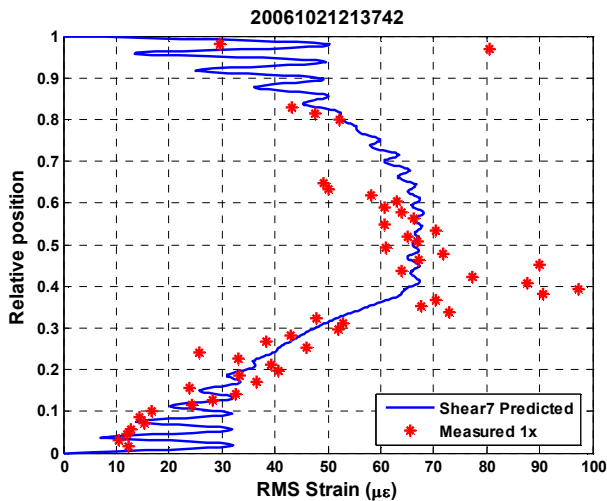


Figure 15. Shear7 v4.5 predicted response using approach 2.

It should also be noted that stress concentration seen in the data was not predicted by the mode superposition method. This is because the changes in mass per unit length leading to wave reflections at the point where strakes begin are not accounted for by the mode superposition method when the eigensolver internal to Shear7 is used, as in this case. The increase in mass per unit length however does lead to an increase in the modal mass and hence to correct lower natural frequencies. An external FEM analysis could be used to improve the mode shapes.

Green's Function Method

Since mode superposition does not account for changes in damping in a local manner and instead applies equal damping over the entire length of the structure, it is desirable to come up with mathematical tools that can handle such a situation. The Green's Function is one way of achieving this goal. The Green's Function of a three zone, damped string under uniform tension is developed below.

Consider the uniform tension damped string shown in Figure 16. It is excited by a point load $Pe^{i\omega t}$ at $x = \xi$. The string is divided into three zones as described in the section on mode superposition.

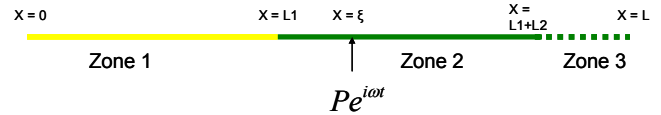


Figure 16. Uniform tension damped string with 3 zones.

The equation governing the motion of the string is:

$$m(x)\ddot{y}(x,t) - Ty''(x,t) + c(x)\dot{y}(x,t) = P\delta(x - \xi)e^{i\omega t} \quad (1.2)$$

where m is the mass per unit length including added mass, T is the uniform tension, c is the damping coefficient, P is the point load magnitude, y is the transverse displacement of the string, x is the distance of any point along the axis from the origin located on left end, δ is the Dirac delta function and ω is the excitation frequency in rad/s. For traveling waves the damping coefficient for a string with uniform mass, tension and damping coefficient is related to the damping ratio (ζ) by equation(1.3).

$$c = 2m\omega\zeta \quad (1.3)$$

Since the mass, tension and damping properties are constant within a zone, we can write a simplified equation of motion for each of the zones as follows:

$$m_j\ddot{y}_j(t) - Ty_j''(t) + c_j\dot{y}_j(t) = P\delta_{j2}\delta(x - \xi)e^{i\omega t} \quad (1.4)$$

where the subscript $j = 1, 2$ or 3 , represents the zone number and δ_{j2} is the Kronecker delta function. Each of the variables or

parameters m , γ and c takes the value associated with the zone denoted by the subscript.

The boundary conditions at $x = 0$ and $x = L$ requires that $y(0,t) = 0$ and $y(L,t) = 0$.

Using the governing equation and the boundary conditions it can be shown that the response in zones 1 and 3 is given by

$$y_1(x,t) = \text{Re}(A_1 \sin(k_1 x) e^{i\omega t}) \quad (1.5)$$

$$y_3(x,t) = \text{Re}(A_3 \sin(k_3(x-L)) e^{i\omega t}) \quad (1.6)$$

where

$$k_j^2 = \frac{m_j \omega^2 + i c_j \omega}{T} \quad (1.7)$$

and A_j are the unknown coefficients that need to be determined.

To develop the solution for zone 2, we assume that the solution is made up of two parts: $y_{2L}(x,t)$ is effective for the part of the zone on the left of point load ($L_1 < x < \xi$) and $y_{2R}(x,t)$ for the part of the zone on the right of point load ($\xi < x < L_1 + L_2$). Each of these solutions will satisfy equation (1.4) with the term on right hand side being zero. Since $y_{2L}(x,t)$ and $y_{2R}(x,t)$ both satisfy linear homogeneous equations, their solutions can be written as follows:

$$y_{2L}(x,t) = \text{Re}[(A_{2L} \sin(k_2 x) + B_{2L} \cos(k_2 x)] e^{i\omega t} \quad (1.8)$$

$$y_{2R}(x,t) = \text{Re}[(A_{2R} \sin(k_2 x) + B_{2R} \cos(k_2 x)] e^{i\omega t} \quad (1.9)$$

There are six unknown coefficients (A_1 , A_3 , A_{2L} , A_{2R} , B_{2L} , B_{2R}) in the solutions presented above. In order to evaluate these unknowns, we must apply the following matching conditions:

$$y_1(L_1, t) = y_{2L}(L_1, t) \quad (1.10)$$

$$y_1'(L_1, t) = y_{2L}'(L_1, t) \quad (1.11)$$

$$y_{2L}(\xi, t) = y_{2R}(\xi, t) \quad (1.12)$$

$$y_{2L}'(\xi, t) - y_{2R}'(\xi, t) = \frac{P e^{i\omega t}}{T} \quad (1.13)$$

$$y_{2R}(L_1 + L_2, t) = y_3(L_1 + L_2, t) \quad (1.14)$$

$$y_{2R}'(L_1 + L_2, t) = y_3'(L_1 + L_2, t) \quad (1.15)$$

By applying the above six matching conditions, we get six simultaneous equations that can be solved to yield the six unknown coefficients.

Once the solution for a point load has been obtained, the solution for a distributed loading can be obtained by linear superposition. The distributed loading is considered to be equivalent to a number of closely spaced point loads. Solutions for each of these point loads must be obtained in the manner described above. The phase of the loads must be taken into account when superposing the solution.

In order to compare the Green's function solution and the mode superposition solution, response is predicted for the 40%

coverage case using the Green's function solution. The distributed excitation loads predicted by Shear7 for each mode (modes 20 to 29) in approach 2 mentioned above is used as the loading in the Green's function solution. Figure 17 shows the spatial variation of the loads for modes 22 and 24. The loads are applied at their corresponding modal frequency. The damping ratio in zone 1 is assumed to be 0.08, for zone 2 it is 0.003 i.e. equivalent to structural damping only and in zone 3 it is assigned a value of 0.03 which is the hydrodynamic damping estimated using Venugopal's hydrodynamic damping model which is used in Shear7.

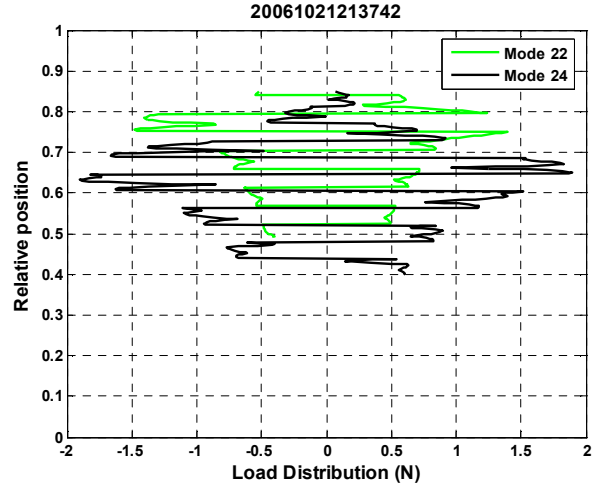


Figure 17. Load distribution for modes 22 and 24 obtained from Shear7.

Figure 18 shows the corresponding responses. Similar responses are calculated for modes 20 to 29. These responses are then averaged using the time sharing concept described earlier with an equal weightage given to all the modes. Figure 19 shows the predicted average response and compares it with the measured response. It is clear that not only the response in the straked region (zone 1) is matched very well but also in the bare region (zone 2) the predicted response is more accurate than that predicted by the mode superposition method. The Green's function method is also able to capture the stress concentration phenomenon seen at the point where the strakes begin.

CONCLUSIONS

The estimated damping ratios for strakes tested during the Gulf Stream Experiments have been presented. In the seven test runs, the damping ratio varied from 0.06 to 0.10 with a mean value of 0.08. The limitations of mode superposition in modeling response of long structures with variable damping have been demonstrated and an alternate method of using Green's functions has been proposed to overcome those limitations.

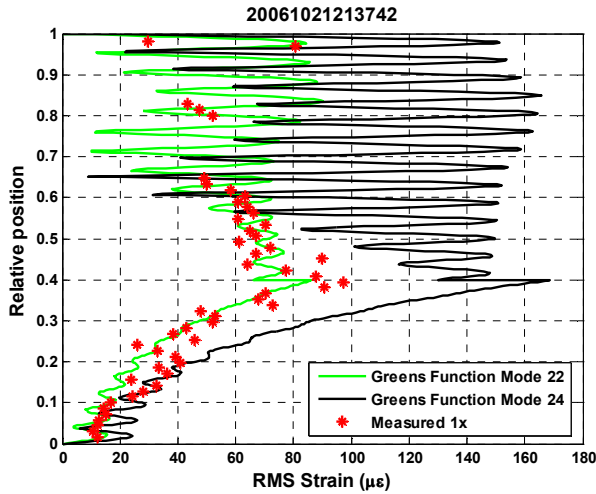


Figure 18. Green's function predicted response for loads applied at modal frequencies of modes 22 and 24. The spatial variation of the loads is shown in Figure 17.

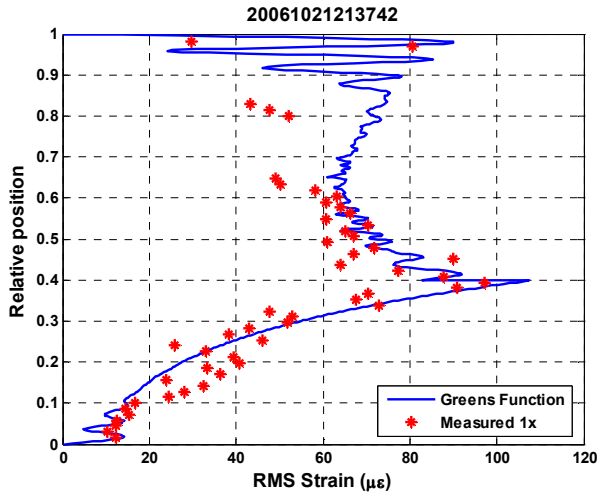


Figure 19. Green's function predicted response.

NOMENCLATURE

A, A_o	Strain [non-dimensional]
K_{sw}, C_{vb}, C_{vh}	Shear7 damping model coefficients
L_1, L_2, L	Length of pipe sections [length]
N	Mode number
P	Load [mass length time ⁻²]
T	Tension [mass length time ⁻²]
U_{mean}	Current [length time ⁻¹]
V_r	Reduced velocity [non-dimensional]
Φ_n	Mode shape
c, c_n	Damping coefficient [mass time ⁻¹]
c_s	Wave speed [length time ⁻¹]

d	Diameter [length]
f, f_1	Frequency [time ⁻¹]
k, k_1, k_2, k_3	Wavenumber [length ⁻¹]
t	Time [time]
x	Distance [length]
δ	Kronecker delta, Dirac delta
ζ	Damping ratio [non-dimensional]
ξ	Distance [length]
ω, ω_n	Frequency [time ⁻¹]

ACKNOWLEDGMENTS

This research was sponsored by the DEEPSTAR Consortium, the Office of Naval Research Ocean Engineering and Marine Systems program (ONR 3210E) and the SHEAR7 JIP. The authors wish to thank the crews of the NUWC Seneca Lake facility and of the R/V F. G. Walton Smith at the University of Miami Rosenstiel School of Marine and Atmospheric Science. The authors are grateful to AIMS International for donating the strakes. The authors also thank Jim Chitwood from Chevron, Robert Knapp from Insensys and Fiberspar. The authors would also like to thank their research team members Vikas Jhingran and Susan Swithenbank of MIT and Dr. Hayden Marcollo of Amog Consulting, Melbourne, Australia.

REFERENCES

- [1] Thomson W. T., 1972, "Theory of Vibration with Applications", Prentice-Hall Inc., Englewood Cliffs, New Jersey, pp 27 Chap. 2
- [2] Vandiver J. K., Swithenbank S. B., Jaiswal V. and Jhingran V., 2006, "Fatigue Damage from High Mode Number Vortex-Induced Vibration", OMAE2006-9240, 25th International Conference on Offshore Mechanics and Engineering, June 2006, Hamburg, Germany.
- [3] Vandiver, J. K. and Chung, T. Y., "Predicted and Measured Response of Flexible Cylinders in Sheared Flows", Proc., ASME Winter Annual Meeting Symposium on Flow-Induced Vibration, Chicago, December 1988.
- [4] Vandiver J. K., Swithenbank S. B., Jaiswal V. and Jhingran V., 2006, "The Effectiveness of Helical Strakes in the Suppression of High Mode-Number VIV", OTC - 18276 - PP, Offshore Technology Conference, 1-4 May 2006, Houston, Texas, USA.
- [5] Venugopal, M., 1996, "Damping and Response of a Flexible Cylinder in Current", PhD thesis, Department of Ocean Engineering, Massachusetts Institute of Technology, Cambridge, USA.
- [6] Vikestad, K., Larsen, C. M. and Vandiver, J. K., 2000, "Norwegian Deepwater Program: Damping of Vortex-Induced Vibrations", OTC 11998, Offshore Technology Conference, 1-4 May 2000, Houston, Texas, USA.
- [7] Gopalkrishnan, R., 1993, Vortex-Induced Forces on Oscillating Bluff Cylinders, Sc. D., Thesis, Department of Ocean Engineering, Massachusetts Institute of Technology and Department of Applied Ocean Physics and Engineering, WHOI, USA.